

Two-Photon Absorption in Anthracene*†

JOHN P. HERNANDEZ‡ AND ALBERT GOLD

Institute of Optics, University of Rochester, Rochester, New York

(Received 10 October 1966)

Two-photon transition rates for molecular and crystalline anthracene are calculated using Pariser's π -electron molecular-orbital wave functions, including configuration interaction. Distinctive polarization dependences and approximate rates are obtained for the 4.94-eV B_{1g} and 5.00-eV A_{1g} molecular states. Frenkel exciton states built from the B_{1g} state are found to be sufficiently red-shifted to account for the absorption observed in the solid. The levels found at 3.48 and 3.58 eV by Fröhlich and Mahr are tentatively identified as the B_g and A_g components, respectively, of the resulting Davydov doublet. Polarization dependences are consistent with available data, and the calculated rate is of reasonable magnitude. An A_{1g} -derived doublet is predicted near 4.8 eV.

I. INTRODUCTION

ALTHOUGH two-photon absorption has been studied more extensively in anthracene than in any other substance,¹⁻¹⁴ detailed understanding of the process in that material is evolving but slowly. Most experiments have detected the absorption of two ruby-laser photons by observing the subsequent blue fluorescence. For a time, the interpretation of these data was obscured by the simultaneous presence of single-photon transitions to weakly absorbing triplet states which decay by triplet-triplet annihilation giving emission in the same spectral range. It is now clear, however, that the double-quantum processes causes a prompt emission with a 26-nsec mean lifetime,⁵ while bimolecular triplet annihilation produces a delayed fluorescence with a mean lifetime of 17 msec.⁵

The final states for the two-photon transitions have not yet been positively identified. Since no known even-parity state of the anthracene molecule exists in the

neighborhood of twice the ruby photon energy (3.6 eV), it has been suggested that the final state is vibronic in character consisting of a small admixture of an even A_{1g} or B_{1g} state into the B_{2u} ^{7,10,14} or B_{3u} ¹⁴ molecular states which lie in the appropriate region of the spectrum. Some workers^{8,9} have conjectured that the final state is of odd parity and that the transition takes place via the A^2 term in the interaction Hamiltonian. However, more careful investigation of this mechanism¹¹ has shown it to predict a transition rate several orders of magnitude smaller than that observed and of the same order as other electric quadrupole and magnetic dipole contributions. Recently, Fröhlich and Mahr¹⁴ have obtained two-photon absorption spectra directly for crystalline anthracene using a neodymium-glass laser and a tunable ultraviolet light source. Their experiment not only traces out the form of the absorption as a function of energy but also gives some information concerning its polarization dependence.

We have undertaken a theoretical study of two-photon absorption in both crystalline and molecular anthracene using Pariser's¹⁵ molecular wave functions. Emphasis is placed on symmetry and related polarization effects throughout. Transitions to the A_{1g} and B_{1g} states which are believed to be at 5.0 and 4.9 eV, respectively, in the free molecule are studied. The even-parity Frenkel exciton states of crystalline anthracene built from these molecular levels have been constructed. It is found that the B_{1g} -derived excitons are red-shifted to the neighborhood of twice the laser frequency. The predicted polarization properties and splitting of the resulting A_g , B_g Davydov doublet are consistent with the measurements of Fröhlich and Mahr. In addition, another doublet of A_{1g} parentage is predicted near 4.8 eV, an as yet unexplored spectral region. We conclude that while two-photon absorption near 3.6 eV may take place to vibronic states in the free molecule, the transitions observed in this neighborhood in the solid are to even-parity excitons derived from the molecular B_{1g} state.

* Research supported in part under contract with the U. S. Army Research Office, Durham, North Carolina.

† Based in part on a thesis submitted by John P. Hernandez in partial fulfillment for the degree of Doctor of Philosophy.

‡ Present address: Department of Physics, University of North Carolina, Chapel Hill, North Carolina.

¹ W. L. Peticolas, J. P. Goldsborough, and K. E. Rieckhoff, *Phys. Rev. Letters* **10**, 43 (1963).

² W. L. Peticolas and K. E. Rieckhoff, *J. Chem. Phys.* **39**, 1347 (1963).

³ W. L. Peticolas, R. Norris, and K. E. Rieckhoff, *J. Chem. Phys.* **42**, 4164 (1965).

⁴ S. Singh and B. P. Stocheff, *J. Chem. Phys.* **38**, 2032 (1963).

⁵ J. L. Hall, D. A. Jennings, and R. M. McClintock, *Phys. Rev. Letters* **11**, 364 (1963).

⁶ E. Evleth and W. L. Peticolas, *J. Chem. Phys.* **41**, 1400 (1964).

⁷ S. Singh, W. L. Jones, W. Siebrand, B. P. Stoicheff, and W. G. Schneider, *J. Chem. Phys.* **42**, 330 (1965).

⁸ M. Iannuzzi and E. Polacco, *Phys. Rev. Letters* **13**, 371 (1964).

⁹ M. Iannuzzi and E. Polacco, *Phys. Rev.* **138**, A806 (1965).

¹⁰ J. M. Worlock, in *Physics of Quantum Electronics*, edited by P. L. Kelley, B. Lax, and P. E. Tannenwald (McGraw-Hill Book Company, Inc., New York, 1966), p. 13.

¹¹ R. Guccione and J. Van Kranendonk, *Phys. Rev. Letters* **14**, 583 (1965).

¹² D. H. McMahon, R. A. Soref, and A. R. Franklin, *Phys. Rev. Letters* **14**, 1060 (1965).

¹³ S. Z. Weisz, A. B. Zahlan, J. Gilreath, R. C. Jarnagin, and M. Silver, *J. Chem. Phys.* **41**, 3491 (1964).

¹⁴ D. Fröhlich and H. Mahr, *Phys. Rev. Letters* **16**, 895 (1966).

¹⁵ R. Pariser, *J. Chem. Phys.* **24**, 250 (1956). Dr. Pariser kindly provided the authors with his unpublished wave functions for $C_{14}H_{10}$.

In Sec. II we give a brief review of the theory of two-photon absorption which is then applied to the A_{1g} and B_{1g} states of the anthracene molecule. The wave functions and energies of even-parity excitons in crystalline anthracene are computed in Sec. III. Section IV presents a calculation of the two-photon transition rate for $\mathbf{k}=0$ excitons, taking the optical anisotropy of the crystal into account. Results and conclusions are summarized in Sec. V. The even-parity exciton band structures are presented in Appendix A, while the details of the molecular wave functions and the computation of molecular matrix elements are given in Appendices B and C, respectively.

II. MOLECULAR TWO-PHOTON ABSORPTION

In the dipole approximation, the two-photon transition rate for excitation of a molecule from initial state $|i\rangle$ to final state $|f\rangle$ is given by¹⁶

$$w_{fi} = (2\pi)^3 (e^2/\hbar c)^2 \hbar (\hbar\omega)^2 F^2 |R_{fi}^{(2)}|^2 g(2\hbar\omega). \quad (1)$$

Here $\hbar\omega$ is the energy of the photons (single beam), F is the photon flux (in photons/cm² sec), and $R_{fi}^{(2)}$, the "second-order matrix element," is

$$R_{fi}^{(2)} = \sum_m \frac{\langle f | \hat{\epsilon} \cdot \mathbf{r} | m \rangle \langle m | \hat{\epsilon} \cdot \mathbf{r} | i \rangle}{E_{mi} - \hbar\omega}, \quad (2)$$

where $|m\rangle$ runs over all intermediate states whose energies relative to $|i\rangle$ are E_{mi} and $\hat{\epsilon}$ is the polarization vector. The phenomenological shape function g is introduced to account for the vibrational structure of the molecular transition and is normalized over the absorption band to

$$\int g(E) dE = 1.$$

If the molecules are imbedded in a dielectric medium, appropriate index of refraction and local field corrections must be made.¹⁶

The anthracene molecule has point symmetry D_{2h} and its ground state transforms according to the totally symmetric representation A_{1g} . Hence, two-photon transitions are allowed to final states of A_{1g} and B_{1g} symmetry. We shall treat these separately below.

A. B_{1g} Final States

Taking x as the long molecular axis and z as the normal to the molecule, we write $\hat{\epsilon}$ in terms of its direction cosines l , m , and n :

$$\hat{\epsilon} = l\hat{x} + m\hat{y} + n\hat{z}.$$

The nonvanishing terms in the second-order matrix

element are then given by

$$R_{B_{1g}A_{1g}}^{(2)} = lm \left[\sum \frac{\langle B_{1g} | x | B_{2u} \rangle \langle B_{2u} | y | A_{1g} \rangle}{E_{B_{2u}A_{1g}} - \hbar\omega} + \sum \frac{\langle B_{1g} | y | B_{3u} \rangle \langle B_{3u} | x | A_{1g} \rangle}{E_{B_{3u}A_{1g}} - \hbar\omega} \right]. \quad (3)$$

In (3), the sums run over all intermediate states of the symmetry type indicated. For a randomly oriented array of molecules, the transition rate will be given by substituting (3) into (1) and averaging lm over all orientations. Letting

$$w_{fi} = A \text{Av}_{\epsilon} |lm|^2,$$

we find that for an unpolarized beam¹⁷

$$\text{Av}_{\text{unpol}} |lm|^2 = 1/36. \quad (4)$$

In the (general) case of elliptically polarized light, we may write

$$\hat{\epsilon} = (x' + ia'y')(1+a^2)^{-1/2}, \quad (5)$$

where x' and y' are arbitrarily oriented in the plane perpendicular to the direction of propagation. Performing the necessary average now gives w as a function of a , the ellipticity parameter,

$$\text{Av}_a |lm|^2 = (a^4 + 4a^2 + 1)/15(1+a^2)^2. \quad (6a)$$

For linearly polarized light, $a=0$ and

$$\text{Av}_{\text{lin}} |lm|^2 = 1/15; \quad (6b)$$

for circularly polarized light, $a=1$ and

$$\text{Av}_{\text{circ}} |lm|^2 = 1/10. \quad (6c)$$

The transition rate relative to that for $a=0$ is plotted in Fig. 1.

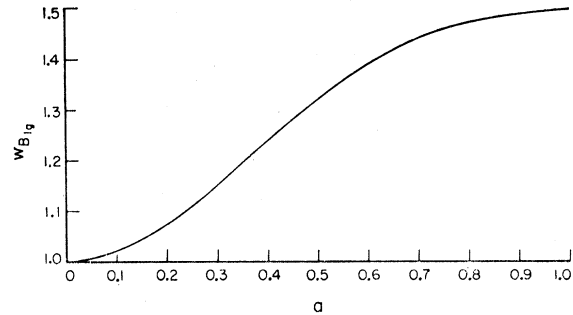


FIG. 1. Relative transition rates for the 4.94-eV B_{1g} state of molecular anthracene as a function of the ellipticity parameter a . ($a=0$ is linear polarization; $a=1$, circular.)

¹⁷ The treatment of unpolarized beams requires a bit of special attention. To account for the independence of the polarizations $\hat{\epsilon}_1$ and $\hat{\epsilon}_2$ of the two photons involved, one writes

$$R_{f_0}^{(2)} = \frac{1}{2} \sum_m (E_{m_0} - \hbar\omega)^{-1} (\langle f | \hat{\epsilon}_1 \cdot \mathbf{r} | m \rangle \langle m | \hat{\epsilon}_2 \cdot \mathbf{r} | g \rangle + \langle f | \hat{\epsilon}_2 \cdot \mathbf{r} | m \rangle \langle m | \hat{\epsilon}_1 \cdot \mathbf{r} | g \rangle),$$

and, after squaring, averages over $\hat{\epsilon}_1$ and $\hat{\epsilon}_2$ direction cosines independently.

¹⁶ See, for example, A. Gold and J. P. Hernandez, Phys. Rev. 139, A2002 (1965).

Clearly, for a B_{1g} final state, the ratio of the two-photon absorption rate for two different states of polarization is a function of *symmetry alone* and can be obtained directly from Eqs. (4) and (6a) or Fig. 1. For example,

$$\frac{w(\text{circ})}{w(\text{lin})} = \frac{3}{2}; \quad \frac{w(\text{lin})}{w(\text{unpol})} = \frac{12}{5}. \quad (6d)$$

Pariser's calculations¹⁵ predict that the lowest B_{1g} state in anthracene is at 4.94 eV. Using an "average energy denominator," we may approximate (3) by

$$R_{B_{1g}A_{1g}} = 2lm \frac{\langle B_{1g} | xy | A_{1g} \rangle}{\bar{E}_{xy} - \hbar\omega}. \quad (7)$$

Equation (7) really defines \bar{E}_{xy} . The "averaging" process and its validity have been discussed elsewhere.¹⁸ We use Pariser's wave functions in (7) taking the lowest allowed molecular transition energy, 3.28 eV, for \bar{E}_{xy} .¹⁰ For a fictitious laser whose energy is $4.9/2 = 2.45$ eV and taking $g(2\hbar\omega) = (0.3 \text{ eV})^{-1}$, we obtain

$$w_{B_{1g}A_{1g}} = 4.75 \times 10^{-47} F^2 \text{ Av} |lm|^2 \text{ sec}^{-1}$$

for the free molecule.

B. A_{1g} Final State

For a transition to a final state $|A_{1g}^*\rangle$ the second-order matrix element is given by

$$R_{A_{1g}A_{1g}}^{(2)} = l^2 \sum \frac{\langle A_{1g}^* | x | B_{3u} \rangle \langle B_{3u} | x | A_{1g} \rangle}{E_{B_{3u}A_{1g}} - \hbar\omega} + m^2 \sum \frac{\langle A_{1g}^* | y | B_{2u} \rangle \langle B_{2u} | y | A_{1g} \rangle}{E_{B_{2u}A_{1g}} - \hbar\omega} + n^2 \sum \frac{\langle A_{1g}^* | z | B_{1u} \rangle \langle B_{1u} | z | A_{1g} \rangle}{E_{B_{1u}A_{1g}} - \hbar\omega}. \quad (8)$$

In the π -electron approximation, the last term in (8) vanishes. To compute absolute transition rates, we now define average energy denominators by

$$w_{A_{1g}A_{1g}} = C \left| \frac{\langle A_{1g}^* | x^2 | A_{1g} \rangle}{\bar{E}_{xx} - \hbar\omega} \right|^2 \text{ Av}_c |l^2 + \lambda B m^2|^2, \quad (9a)$$

where

$$C = (2\pi)^3 (e^2/\hbar c)^2 \hbar (\hbar\omega)^2 F^2 g(2\hbar\omega), \quad (9b)$$

$$\lambda = (\bar{E}_{xx} - \hbar\omega) / (\bar{E}_{yy} - \hbar\omega), \quad (9c)$$

and

$$B = \frac{\langle A_{1g}^* | y^2 | A_{1g} \rangle}{\langle A_{1g}^* | x^2 | A_{1g} \rangle}. \quad (9d)$$

The necessary angular averages may be performed to yield

$$\text{Av}_{\text{unpol}} |l^2 + \lambda B m^2|^2 = \frac{1}{9} (1 + \lambda^2 B^2) \quad (10)$$

¹⁸ H. B. Bebb and A. Gold, Phys. Rev. 143, 1 (1966).

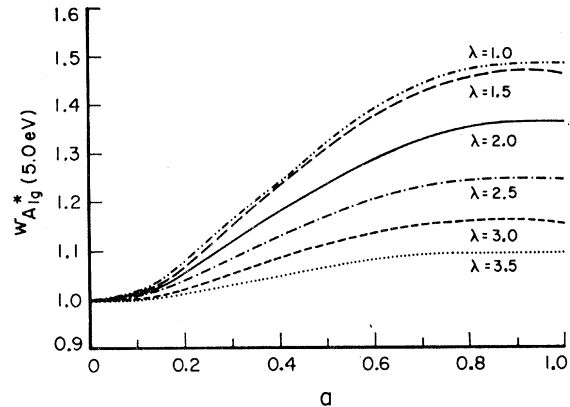


FIG. 2. Relative transition rates for the 5.00-eV A_{1g} state of molecular anthracene as a function of the ellipticity parameter a . The parameter λ is defined and discussed in the text.

and

$$\text{Av}_a |l^2 + \lambda B m^2|^2 = (1/15)(1 + a^2)^{-2} [(3a^4 + 2a^2 + 3) \times (1 + \lambda^2 B^2) + \frac{1}{8} \lambda B (21a^4 - 101a^2 + 16)]. \quad (11a)$$

two special cases of interest are

$$\text{Av}_{\text{lin}} |l^2 + \lambda B m^2|^2 = (3\lambda^2 B^2 + 2\lambda B + 3)/15, \quad (11b)$$

$$\text{Av}_{\text{circ}} |l^2 + \lambda B m^2|^2 = 2(\lambda^2 B^2 - \lambda B + 1)/15. \quad (11c)$$

Pariser's calculations predict the lowest excited A_{1g} state to be at 5.00 eV. Using his wave functions we have computed $B(5.0 \text{ eV}) = -0.844$. The predicted transition rate for this state ($\hbar\omega = 2.5 \text{ eV}$) is

$$w_{A_{1g}A_{1g}} = 2.8 \times 10^{-50} F^2 \text{ Av}_c |l^2 + \lambda B(5.0)m^2|^2 \text{ sec}^{-1}. \quad (11d)$$

Approximating λ by taking the lowest coupling excited state energies as \bar{E}_{xx} and \bar{E}_{yy} ^{15,10} in (9c) gives

$$\lambda = \frac{(E_{B_{3u}} - \hbar\omega)}{(E_{B_{2u}} - \hbar\omega)} = \frac{5.24 - 2.5}{3.28 - 2.5} = 3.5.$$

However, we choose to regard λ as a parameter and plot $w(a)$ in the range $\lambda = 1$ to 3.5 in Fig. 2. Ratios of absorption for different polarization states for various values of λ are presented in Table I. Despite the parametrization, the A_{1g} final state is clearly distinguishable from B_{1g} . However, in this case $w(a)$ is not purely symmetry determined as it was for B_{1g} states. Note that the A_{1g} transition is appreciably weaker than that to the B_{1g} state.

TABLE I. Some polarization ratios for the 5.00-eV A_{1g} state of anthracene as a function of λ (see text).

λ	1.0	1.5	2.0	2.5	3.0	3.5
$\frac{w(\text{circular})}{w(\text{linear})}$	1.48	1.46	1.36	1.24	1.16	1.09
$\frac{w(\text{linear})}{w(\text{unpolarized})}$	1.21	1.22	1.27	1.33	1.39	1.43

III. EVEN-PARITY EXCITONS

Neglecting exchange and overlap, Frenkel-model exciton states of wave vector \mathbf{k} for a crystal having N unit cells each containing two translationally inequivalent molecules occur in Davydov doublets $\chi_{\mathbf{k}\pm}$, which may be written^{19,20}

$$\chi_{\mathbf{k}\pm} = (2N)^{-1/2} \sum_{l=1}^N [\Phi_i(\mathbf{r}-\mathbf{R}_{l1}) \prod'_{m\alpha} \Phi_o(\mathbf{r}-\mathbf{R}_{m\alpha}) \pm e^{i\mathbf{k}\cdot\mathbf{R}'} \Phi_i(\mathbf{r}-\mathbf{R}_{l1}-\mathbf{R}') \prod'_{m\alpha} \Phi_o(\mathbf{r}-\mathbf{R}_{m\alpha})] e^{i\mathbf{k}\cdot\mathbf{R}_{l1}}. \quad (12)$$

In Eq. (12), $\Phi_i(\mathbf{r}-\mathbf{R}_{l1})$ is the wave function for the i th excited state of the molecule at site 1 in the l th cell. \mathbf{R}' is the vector connecting the two inequivalent molecules in the cell. $\Phi_o(\mathbf{r}-\mathbf{R}_{m\alpha})$ is the ground-state wave function of the α th molecule in cell m , and the prime on the product reminds us to exclude the excited molecule. The $+$ and $-$ in our case correspond to A_g and B_g excitons in the crystal of C_{2h} symmetry.

The intermolecular interaction Hamiltonian is the sum of the pairwise interactions

$$H_{12} = \sum_{I,J} \frac{e^2}{|\mathbf{R}_{1I}-\mathbf{R}_{2J}|} + \sum_{i,j} \frac{e^2}{|\mathbf{r}_{1i}-\mathbf{r}_{2j}|} - \sum_{I,j} \frac{e^2}{|\mathbf{R}_{1I}-\mathbf{r}_{2j}|} - \sum_{J,i} \frac{e^2}{|\mathbf{R}_{2J}-\mathbf{r}_{1i}|}, \quad (13)$$

where I runs over the carbon nuclei and i over the π -electrons of molecule 1, and similarly for J and j in molecule 2. Neglecting exchange and overlap,²¹ the first-order exciton energies for high-symmetry directions are given by^{19,22}

$$\mathcal{E}_i(\mathbf{k}) = E_i - E_o + D_i + \Delta_i(\mathbf{k}) \pm d_i(\mathbf{k}), \quad (14)$$

where

$$D_i = \sum_{l=1}^N \sum_{\alpha=1}^2 (\langle i01,gl\alpha | H_{12} | i01,gl\alpha \rangle - \langle g01,gl\alpha | H_{12} | g01,gl\alpha \rangle), \quad (15a)$$

$$\Delta_i(\mathbf{k}) = \sum_{l=1}^N \langle i01,gl1 | H_{12} | g01,il1 \rangle \cos \mathbf{k} \cdot \mathbf{R}_{l1}, \quad (15b)$$

$$d_i(\mathbf{k}) = \sum_{l=0}^N \langle i01,gl2 | H_{12} | g01,il2 \rangle \cos \mathbf{k} \cdot \mathbf{R}_{l2}. \quad (15c)$$

Here, for example, $\langle i01,gl\alpha |$ means the product of the wave function of molecule 1 in the i th excited state

¹⁹ R. S. Knox, *Theory of Excitons* (Academic Press Inc., New York, 1963).

²⁰ A. S. Davydov, *Theory of Molecular Excitons* (McGraw-Hill Book Company, Inc., New York, 1962).

²¹ R. Silbey, J. Jortner, and S. A. Rice, *J. Chem. Phys.* **42**, 1515 (1965).

²² Equations (12), (14), and (15) are not completely general, but do contain all nonvanishing terms for the wave vector directions given in Appendix A; see discussion on p. 30ff of Ref. 19.

located at position 1 in the 0th unit cell with that of molecule 2 in the ground (g) state at position α in the l th unit cell; $\mathbf{R}_{l\alpha}$ is the vector from molecule 1 to molecule 2. Physically, the energy is that of a free molecule perturbed by intermolecular Coulomb interaction D , and by terms Δ , representing the transfer of energy to equivalent sites, and d , representing transfer to inequivalent molecules.

Equations (15) are evaluated by making a multipole expansion of H_{12} . For even-parity states the lowest-order nonvanishing term is the quadrupole-quadrupole interaction. It is also necessary to include the second-order van der Waals interactions in the energy shifts. This is obtained by making the following replacement in Eqs. (15):

$$H_{12} \rightarrow - \sum_{m,n} \frac{H_{12} |m,n\rangle \langle m,n| H_{12}}{E_m + E_n - E_{ig}}, \quad (16)$$

where $|m\rangle$ and $|n\rangle$ run individually over complete sets of molecular states at the appropriate site.

Several calculations of this type have been performed (for odd-parity states), and so we shall not reproduce the computational details here. The odd excitons of anthracene have been treated recently by Davydov and Sheka²³ and by Sibley, Jortner, and Rice.²¹ The latter calculation used Pariser's molecular wave functions but gave only ambiguous agreement with experiment. The computed value of the oscillator strength, 0.4, was compared to an experimental value of 0.1. Sibley *et al.*²¹ consequently scaled all matrix elements to give agreement with the measured oscillator strength. However, Brodin and Marisova²⁴ have recently repeated the measurements using improved techniques and find an oscillator strength of 0.4 and a polarization ratio of 7. The latter is in good agreement with the value calculated using an oriented gas model of the crystal.²⁴ This recent work lends strong credence both to the use of the wave functions and to the adequacy of the zero-order rigid-gas model for predicting polarization effects. Furthermore, it indicates that exchange makes only a small ($\sim 10\%$) contribution to the shifts and splitting, rendering our neglect of it reasonable.²¹

The first-order contributions D , Δ , and d have been summed explicitly over the crystal. It is found that contributions from sites separated by more than $40a_0$ are negligible.²⁵ A maximum value of the van der Waals energy is computed by replacing all energy denominators in (16) with the smallest one having nonvanishing matrix elements. A "reasonable" estimate is obtained by taking an average energy denominator of 12 eV (about twice the ionization potential). This gives a reasonable ground-state binding energy of 0.12 eV. We

²³ A. S. Davydov and E. F. Sheka, *Phys. Status Solidi* **11**, 877 (1965).

²⁴ M. S. Brodin and S. V. Marisova, *Opt. Spectry.* **19**, 132 (1965).

²⁵ For further detail see J. P. Hernandez, thesis, University of Rochester, 1966 (unpublished).

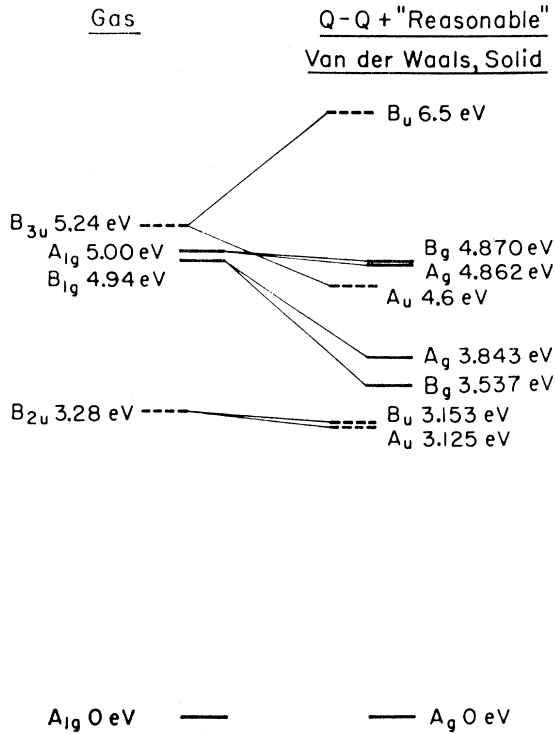


FIG. 3. Low-lying singlet states of anthracene. The odd-parity states are located experimentally throughout. Even-parity states in the gas are those predicted by Pariser. Even-parity states in the solid are calculated using only the quadrupole-quadrupole ($Q-Q$) interaction.

find that the first-order terms dominate the splittings and \mathbf{k} dependence, but the van der Waals energy dominates the over-all shifts.

The shifts are all to the red. The B_g state derived from the 4.9 eV B_{1g} molecular state lies below the A_g state, while for the A_{1g} molecular level the Davydov doublet is in the reverse order. The first-order, quadrupole-quadrupole ($Q-Q$) interactions for $\mathbf{k}=0$ excitons are shown in Fig. 3. Adding the maximum van der Waals (vdW) energy, we obtain the results of Fig. 4, which are also presented in Table II to facilitate comparison of various terms. The "reasonable" van der Waals interaction is included in Fig. 5. This places the B_{1g} -

TABLE II. Contributions to the $\mathbf{k}=0$ exciton energies for A_{1g} and B_{1g} states. The A_g energy is $D+\Delta+d$ while that for B_g is $D+\Delta-d$.

State	4.94 eV	5.00 eV	Ground state
Maximum van der Waals interaction (in eV)			
D	-2.971	-1.054	-0.221
Δ ($k=0$)	+0.058	-0.001	
d ($k=0$)	-0.179	+0.0009	
$Q-Q$, First order (in eV)			
D	-0.565	-0.023	0
Δ ($k=0$)	-0.142	+0.002	
d ($k=0$)	+0.194	-0.004	

derived, two-photon-accessible B_g and A_g states at 3.5 and 3.8 eV, respectively. The band structure of the even exciton states for high-symmetry directions of \mathbf{k} is given in Appendix A.

Comparing Fig. 5 to the results of Fröhlich and Mahr,¹⁴ we identify their absorption bands with the B_{1g} exciton doublet. The predicted splitting is too large by 0.2 eV and the shifts too small by a like amount, but these discrepancies are well within the bounds of confidence that can be placed on our numerical results. Specifically, we assign the peak at 3.48 eV to the B_g exciton and that at 3.58 eV to the exciton of A_g symmetry. We shall discuss this assignment, based on polarization data, in the next section.

IV. TWO-PHOTON ABSORPTION BY EXCITONS

In computing the rate of two-photon absorption by excitons in the monoclinic, optically biaxial anthracene crystal, it is necessary to account for anisotropy. Consider light incident perpendicular to the ab cleavage plane with polarization $\hat{\epsilon} = \hat{a} \cos\alpha + \hat{b} \sin\alpha$. The \hat{b} polarized component continues through the crystal unrefracted. On the other hand, using Nakada's²⁶ measured values of the index as a function of direction, shown in Fig. 6, one finds that the \hat{a} component is refracted to $6.2 \pm 1.8^\circ$. Within a thin crystal, the two beams over-

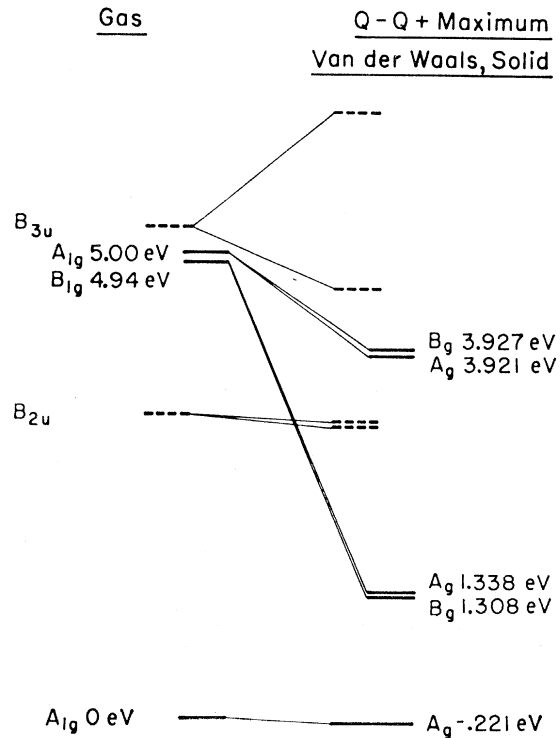


FIG. 4. Even-parity exciton states obtained using a maximum van der Waals interaction in addition to the quadrupole-quadrupole terms. See also Fig. 3.

²⁶ I. Nakada, J. Phys. Soc. Japan 17, 113 (1962).

lap giving constantly changing elliptical polarization. For example, linearly polarized light with $\alpha=45^\circ$ becomes circularly polarized after traveling through 3000 Å. Thin samples or small crystallites are thus not amenable to detailed analysis for general polarization and we shall restrict our attention to linear polarization where $\alpha=0, \pm\pi/2$ or to cases in which the crystal is "thick," i.e., (thickness)/(incident beam diameter) > 50 . In the former case there is only one plane polarized beam within the crystal, while in the latter the two beams are nonoverlapping through most of the absorbing volume. The transition rate in the crystal is now given approximately by¹⁶

$$w_{ji} = C \left(\frac{n_\omega^2(\hat{\epsilon}) + 2}{3} \right)^4 \frac{|R_{ji}^{(2)}|^2}{n_\omega^2(\hat{\epsilon})}, \quad (17a)$$

where

$$C = (2\pi)^3 (e^2/\hbar c)^2 \hbar(\hbar\omega)^2 F^2 g(2\hbar\omega), \quad (17b)$$

and $n_\omega(\hat{\epsilon})$ is the index of the medium for light of frequency ω polarized in the $\hat{\epsilon}$ direction. The polarization vector is that inside the crystal, which because of the refraction described above is given by²⁶

$$\hat{\epsilon} = (\hat{a} \cos 6.2^\circ + \hat{c}' \sin 6.2^\circ) \cos \alpha + \hat{b} \sin \alpha \equiv \hat{a}' \cos \alpha + \hat{b} \sin \alpha.$$

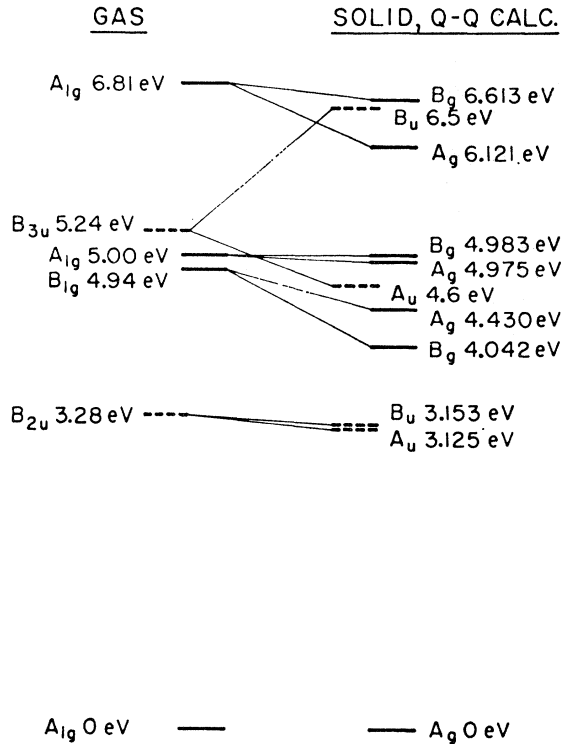


FIG. 5. Even-parity exciton states obtained using a reasonable estimated van der Waals interaction in addition to the quadrupole-quadrupole terms. The ground state is taken as a datum. See also Fig. 3.

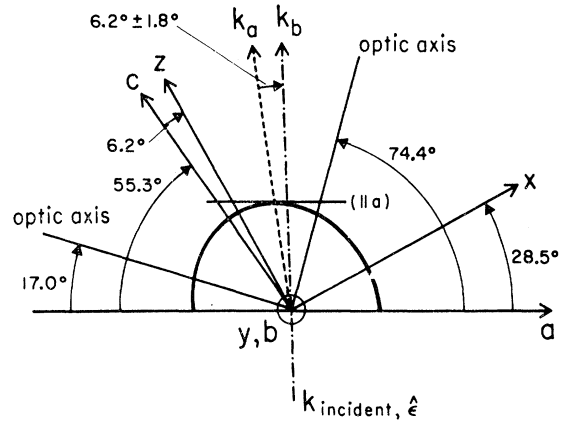


FIG. 6. Important crystallographic and optical axes in crystal anthracene (after Nakada, Ref. 26).

Then, for B_θ states,

$$R_{B_\theta A_\theta}^{(2)} = \sin \alpha \cos \alpha \left[\sum \frac{\langle B_\theta | \hat{a}' \cdot \mathbf{r} | A_u \rangle \langle A_u | \hat{b} \cdot \mathbf{r} | A_\theta \rangle}{E_{A_u A_\theta} - \hbar \omega} + \sum \frac{\langle B_\theta | \hat{b} \cdot \mathbf{r} | B_u \rangle \langle B_u | \hat{a}' \cdot \mathbf{r} | A_\theta \rangle}{E_{B_u A_\theta} - \hbar \omega} \right].$$

In analogy to Eq. (7), we define \bar{E}_{ab} by

$$R_{B_\theta A_\theta}^{(2)} = 2(\sin \alpha \cos \alpha) \langle B_\theta | (\hat{a}' \cdot \mathbf{r})(\hat{b} \cdot \mathbf{r}) | A_\theta \rangle / (\bar{E}_{ab} - \hbar \omega).$$

For A_θ states,

$$R_{A_\theta A_\theta}^{(2)} = \cos^2 \alpha \sum \frac{\langle A_\theta^* | \hat{a}' \cdot \mathbf{r} | B_u \rangle \langle B_u | \hat{a}' \cdot \mathbf{r} | A_\theta \rangle}{E_{B_u A_\theta} - \hbar \omega} + \sin^2 \alpha \sum \frac{\langle A_\theta^* | \hat{b} \cdot \mathbf{r} | A_u \rangle \langle A_u | \hat{b} \cdot \mathbf{r} | A_\theta \rangle}{E_{A_u A_\theta} - \hbar \omega}.$$

We now define \bar{E}_{aa} and \bar{E}_{bb} by

$$R_{A_\theta A_\theta}^{(2)} = \cos^2 \alpha \frac{\langle A_\theta^* | (\hat{a}' \cdot \mathbf{r})^2 | A_\theta \rangle}{\bar{E}_{aa} - \hbar \omega} + \sin^2 \alpha \frac{\langle A_\theta^* | (\hat{b} \cdot \mathbf{r})^2 | A_\theta \rangle}{\bar{E}_{bb} - \hbar \omega}.$$

Since the lowest-energy intermediate states for \hat{b} - and \hat{a} -polarized light are the components of the B_{2u} -derived doublet at 3.125 and 3.153 eV, respectively, we shall take all average energies equal to 3.13 eV in our numerical computations.

Using the wave function of Eq. (12) and Nakada's values of the index, one obtains the following transition rates (at $\mathbf{k}=0$) for B_{1g} -derived states:

$$w_{B_\theta A_\theta} = 7.4 \times 10^{-48} F^2 \sin^2 \alpha \cos^2 \alpha \sec^{-1} \quad (18a)$$

and

$$w_{A_\theta A_\theta} = 6.5 \times 10^{-49} F^2 |\cos^2 \alpha + 0.70 \mu \sin^2 \alpha|^2 \sec^{-1}. \quad (18b)$$

In obtaining (18) we have taken $\hbar\omega = 1.78$ eV and $g(E) = (0.6 \text{ eV})^{-1}$ from the spectra of Ref. 14. It should be pointed out that the angular dependence of B_θ states is a function of symmetry alone. The A_θ angular de-

pendence is not a function of symmetry alone but depends on a parameter $\mu = (\bar{E}_{aa} - \hbar\omega) / (\bar{E}_{bb} - \hbar\omega)$ which we will take equal to 1. To compare the magnitude of the absorption with Ref. 14, we take $\alpha = \pm\pi/2$ (*b*-polarized) for the high-energy state (A_g)²⁷ and obtain $w/F^2 = 3 \times 10^{-49}$ compared with the observed value 2×10^{-49} . For the low-energy state, direct comparison is only possible for the trivial case $\alpha = \pm\pi/2$ where both predicted and observed absorption vanishes. These results are consistent with the assignment of an A_g exciton to the high-energy peak and one of B_g symmetry to the low-energy band. Unfortunately, Fröhlich and Mahr's use of multiple internal reflection to increase beam intensity in the crystal makes it impossible to compare polarization predictions for $\alpha \neq \pi/2$ with their data.

A search for the A_{1g} -derived doublet predicted near 4.8 eV would be most informative. The transition rates calculated for these states are

$$w_{B_g A_g} = 3.26 \times 10^{-49} F^2 \sin^2 \alpha \cos^2 \alpha \text{ sec}^{-1} \quad (19a)$$

and

$$w_{A_g A_g} = 3.70 \times 10^{-51} F^2 |\cos^2 \alpha - 10.9 \mu \sin^2 \alpha|^2 \text{ sec}^{-1}. \quad (19b)$$

In obtaining (19) we used $\hbar\omega = 2.4$ eV, $g(2\hbar\omega) = (0.6 \text{ eV})^{-1}$; the parameter μ defined previously is estimated to be near 1. The B_g exciton is predicted at higher energy, but the splitting (see Fig. 5) is expected to be quite small.

V. SUMMARY AND DISCUSSION

We have computed the polarization dependence for two-photon absorption to even-parity electronic states in molecular anthracene. Transitions to A_{1g} and B_{1g} states near 5 eV should be observable and readily distinguishable. The B_{1g} is predicted to be appreciably stronger than the A_{1g} .

The lowest even-parity exciton states have been calculated. Substantial red shifts are found and the two bands found by Fröhlich and Mahr at 3.48 and 3.58 eV are identified as the B_g and A_g excitons derived from the molecular B_{1g} state, respectively.

Both the polarization dependence and order of magnitude of the absolute strength are in agreement with available data. An A_{1g} -derived Davydov doublet is predicted near 4.8 eV.

Several workers have suggested that two-photon absorption in anthracene takes place through the agency of vibronic mixing of even-parity states into odd levels which lie near 3.6 eV.^{7,10,14} Even though the preceding calculations indicate that excitons are in fact responsible for the principal absorption in the crystal, vibronic mixing remains of interest in considering gas-

phase or solution spectra and perhaps for the weak crystalline absorption observed at 3.18 eV.⁷ Vibronic coupling can take place to both the 3.28-eV B_{2u} and the B_{3u} states which Pariser predicts at about 3.7 eV, and both A_{1g} and B_{1g} states may be mixed into either of these by appropriate odd-parity vibrations.

For a given odd-parity "host" level and a specific even-parity "guest," an absorption head will begin one vibrational quantum above the pure electronic energy of the mixed state. Each of the possible absorption bands thus constructed will, however, retain the polarization properties of the even state which is mixed in, and, hence, the results of Sec. II may be used in sorting them out. The strength of the vibronic bands will be diminished by the order of the square of the vibronic coupling constant (typically a factor of about 100) from that of corresponding purely electronic transitions. The ratio of 70 reported for laser-induced fluorescence found in crystalline anthracene to that in the liquid¹² is a possible manifestation of this difference between exciton and vibronic processes.

In the gas phase, vibronic transitions should be clearly identifiable by the characteristic $\coth(\hbar\omega'/kT)$ temperature dependence of the integrated transition rate, where ω' is the frequency of the "mixing" vibration. Experimental measurements of the temperature dependence will be most valuable. Unfortunately, the high energy of intramolecular vibrations ($\sim 1000 \text{ cm}^{-1}$) does not permit a variation sufficient for clear observation in the crystal below the melting point.

Another possible complication has been pointed out by Honig, Jortner, and Szöke.²⁸ They note that vibronic coupling in the *intermediate states* may permit two-photon transitions to the odd-parity molecular states themselves. They calculate such a rate in benzene and find its order of magnitude comparable to what one might expect from final-state vibronic coupling of the type just discussed. Regrettably, the simplicity of the polarization dependence is in general destroyed in this case, and reasonable symmetry predictions can be made only if a single intermediate state fortuitously dominates.

ACKNOWLEDGMENTS

We wish to express our sincere gratitude to Dr. R. Pariser for providing us with his unpublished anthracene wave functions and to Professor M. P. Givens, Professor H. Mahr, and Dr. J. H. Hall for useful discussions.

APPENDIX A: EXCITON BAND STRUCTURE

The energy of the exciton states as a function of wave vector is given in Tables III and IV. \mathbf{k} is the value of the wave vector in units of π/a , π/b , or π/c , respectively, for the three sets of entries in each table. The energies

²⁷ In the case of two beams of different energy but parallel polarization, the second-order matrix element simply becomes

$$R_{fg}^{(2)} = \sum_m \langle f | \hat{\mathbf{e}} \cdot \mathbf{r} | m \rangle \langle m | \hat{\mathbf{e}} \cdot \mathbf{r} | g \rangle [(E_{m0} - \hbar\omega_1)^{-1} + (E_{m0} - \hbar\omega_2)^{-1}].$$

²⁸ B. Honig, J. Jortner, and A. Szöke (to be published).

TABLE III. Band structure of the B_{1g} -derived exciton states.

k_a	$E(A_g)$	$E(B_g)$	$E(A_g)$	$E(B_g)$
0	51.1	-336.0	23.3	-281.8
0.1	48.5	-333.7	21.3	-279.9
0.2	40.7	-326.9	15.3	-274.5
0.3	28.0	-315.6	5.5	-265.6
0.4	10.9	-300.3	-7.8	-253.4
0.5	-10.2	-281.3	-24.3	-238.3
0.6	-34.7	-259.2	-43.6	-220.8
0.7	-61.8	-234.6	-64.9	-201.3
0.8	-90.6	-207.9	-87.8	-180.3
0.9	-120.4	-179.7	-111.3	-158.1
1.0	-150.3	-150.3	-135.0	-135.0
k_b				
0.1	56.8	-327.8	28.8	-274.6
0.2	72.0	-303.8	46.6	-253.9
0.3	91.9	-265.8	63.1	-221.2
0.4	112.3	-216.5	83.2	-178.8
0.5	130.0	-159.2	101.2	-129.6
0.6	143.0	-98.2	115.3	-77.4
0.7	149.1	-37.9	123.5	-26.1
0.8	145.7	17.7	123.2	20.7
0.9	130.6	65.5	112.8	60.5
1.0	103.6	103.6	91.6	91.6
k_c				
0.1	51.9	-335.9	24.0	-281.7
0.2	54.1	-335.6	26.2	-281.4
0.3	57.6	-335.1	29.6	-281.0
0.4	62.0	-334.5	33.9	-280.4
0.5	66.9	-333.8	38.6	-279.8
0.6	71.8	-333.1	43.3	-279.2
0.7	76.1	-332.5	47.6	-278.6
0.8	79.6	-332.0	51.0	-278.2
0.9	81.9	-331.7	53.2	-277.9
1.0	82.6	-331.6	53.9	-277.8

TABLE IV. Band structure of the A_{1g} -derived exciton states.

k_a	$E(A_g)$	$E(B_g)$	$E(A_g)$	$E(B_g)$
0	-1.21	6.09	-1.34	5.57
0.1	-1.14	6.05	-1.27	5.53
0.2	-0.98	5.93	-1.11	5.42
0.3	-0.70	5.73	-0.84	5.23
0.4	-0.31	5.47	-0.46	4.99
0.5	0.16	5.15	-0.01	4.69
0.6	0.69	4.78	0.50	4.35
0.7	1.25	4.36	1.03	3.96
0.8	1.82	3.92	1.57	3.55
0.9	2.39	3.44	2.11	3.10
1.0	2.93	2.93	2.62	2.62
k_b				
0.1	-1.31	5.93	-1.42	5.42
0.2	-1.60	5.48	-1.67	5.02
0.3	-1.99	4.77	-2.00	4.38
0.4	-2.37	3.85	-2.30	3.56
0.5	-2.70	2.78	-2.56	2.60
0.6	-2.94	1.64	-2.73	1.57
0.7	-3.05	0.51	-2.79	0.55
0.8	-2.98	-0.54	-2.69	-0.40
0.9	-2.68	-1.44	-2.39	-1.22
1.0	-2.16	-2.16	-1.89	-1.89
k_c				
0.1	-1.21	6.09	-1.33	5.57
0.2	-1.23	6.09	-1.35	5.57
0.3	-1.27	6.09	-1.38	5.56
0.4	-1.31	6.10	-1.41	5.57
0.5	-1.36	6.11	-1.45	5.58
0.6	-1.41	6.11	-1.49	5.58
0.7	-1.45	6.12	-1.52	5.59
0.8	-1.49	6.13	-1.55	5.60
0.9	-1.51	6.13	-1.58	5.60
1.0	-1.52	6.13	-1.57	5.60

are given in meV. The second and third columns are the calculation of the Q - Q interaction. The fourth and last columns are the "reasonable" van der Waals interaction plus the Q - Q calculation. Note that while the positions of the bands as a whole are sensitive to the van der Waals energy, the shapes and splittings are not.

For this Appendix

$$E_i^{\pm}(\mathbf{k}) = \Delta_i(\mathbf{k}) \pm d_i(\mathbf{k}),$$

with the zero of energy taken at $E_i - E_0 + D_i$ as defined in the text. k_a is along $\mathbf{b} \times \mathbf{c}$, k_b along $\mathbf{c} \times \mathbf{a}$, and k_c along $\mathbf{a} \times \mathbf{b}$.

APPENDIX B: WAVE FUNCTIONS

For completeness we include Pariser's¹⁵ results for the two lowest-energy even-parity states of the anthracene molecule. Beginning with $2p\pi$ carbon functions, χ one constructs molecular orbitals ϕ .

$$\phi_{\lambda}^{\pm} = \sum_{\mu=1}^7 c_{\lambda\mu}^{\pm} (\chi_{\mu} \pm \chi_{\mu}'), \quad (\text{B1})$$

where λ labels the molecular orbital and μ the carbon atoms as in Fig. 7. For the Hamiltonian

$$H = \sum_{\alpha=1}^{14} (H_{\text{core}})_{\alpha} + \sum_{p>q} \frac{e^2}{r_{pq}}, \quad (\text{B2})$$

where p and q run over π -electrons and only nearest-neighbor contributions are considered,

$$H\phi_{\lambda}^{\pm} = (E_0 + k_{\lambda} \pm \beta)\phi_{\lambda}^{\pm}, \quad (\text{B3})$$

where E_0 is the energy of a $2p\pi$ electron for an isolated carbon atom, β is the nearest-neighbor resonance integral, and k_{λ}^{\pm} are given in Table V. The coefficients for the molecular orbitals have been calculated²⁹ and are also given in Table VI. The symmetry classes of the

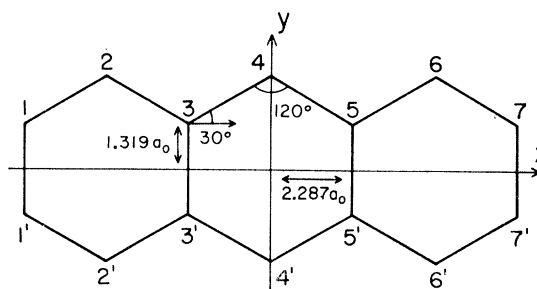


FIG. 7. Geometry of the anthracene molecule.

²⁹ R. McWeeny, Proc. Phys. Soc. (London) A65, 839 (1952).

TABLE V. The energy parameters k_λ^\pm and coefficient $c_{\lambda\mu}^\pm$ for anthracene according to Pariser (Ref. 15). For definitions see text.

$\mu \backslash \lambda$	1	2	3	4	5	6	7	k_λ
1 ⁺	0.15194	0.21488	0.36683	0.30389	0.36683	0.21488	0.15194	2.4142
2 ⁺	0.28867	0.28867	0.28867	0	-0.28867	-0.28867	-0.28867	2.0000
1 ⁻	0.11629	0.28076	0.28076	0.39705	0.28076	0.28076	0.11629	1.4142
3 ⁺	0.40626	0.16828	-0.16828	-0.23798	-0.16828	0.16828	0.40626	1.4142
2 ⁻	0.20412	0.40825	0.20412	0	-0.20412	-0.40825	-0.20412	1.0000
4 ⁺	0.35355	0	-0.35355	0	0.35355	0	-0.35355	1.0000
3 ⁻	0.21987	0.31094	-0.09107	-0.43973	-0.09107	0.31094	0.21987	0.4142
7 ⁻	0.15194	-0.21488	0.36683	-0.30389	0.36683	-0.21488	0.15194	-2.4142
6 ⁻	0.28867	-0.28867	0.28867	0	-0.28867	0.28867	-0.28867	-2.0000
7 ⁺	0.11629	-0.28076	0.28076	-0.39705	0.28076	-0.28076	0.11629	-1.4142
5 ⁻	0.40626	-0.16828	-0.16828	0.23798	-0.16828	-0.16828	0.40626	-1.4142
6 ⁺	0.20412	-0.40825	0.20412	0	-0.20412	0.40825	-0.20412	-1.0000
4 ⁻	0.35355	0	-0.35355	0	0.35355	0	-0.35355	-1.0000
5 ⁺	0.21987	-0.31094	-0.09107	0.43973	-0.09107	-0.31094	0.21987	-0.4142

TABLE VI. Configuration interaction coefficient for anthracene. The notation is that of Ref. 15.

	E (eV)	Anthracene wave functions					
		(0)	(3 ⁻ 5 ⁻ -3 ⁺ 5 ⁺)	(4 ⁺ 6 ⁺ -2 ⁻ 4 ⁻)	(3 ⁻ 7 ⁻ -1 ⁺ 7 ⁺)	(1 ⁻ 5 ⁻ -3 ⁺ 7 ⁺)	(2 ⁺ 6 ⁺ -2 ⁻ 6 ⁻)
A_{1g}	0	0.99618	-0.00801	-0.07416	-0.00895	0.03473	-0.02780
	5.00	0.05792	-0.63796	0.73320	0.11964	-0.19282	0.02395
		(3 ⁻ 6 ⁺ -2 ⁻ 5 ⁺)		(4 ⁺ 5 ⁻ -3 ⁺ 4 ⁻)		(1 ⁻ 6 ⁺ -2 ⁻ 7 ⁺)	
B_{1g}	4.94	0.96114		0.02412		-0.27500	

molecular orbitals are

$$\phi^+: \lambda \text{ odd, } b_{1u}; \lambda \text{ even, } b_{2g};$$

$$\phi^-: \lambda \text{ odd, } b_{3g}; \lambda \text{ even, } a_{1u}.$$

The lowest-energy configuration doubly occupies the seven molecular orbitals characterized by positive k_λ values.

Configurations are built by antisymmetrizing the occupied molecular orbitals. The lowest-energy configuration is

$$V_0 = (14!)^{-1/2} \sum_P (-1)^P P \phi_1(1) \alpha \phi_1(2) \beta \phi_2(3) \times \alpha \phi_2(4) \beta \cdots \phi_7(14) \beta \equiv (1\bar{1}, 2\bar{2}, \cdots, \bar{7}), \quad (\text{B4})$$

where P is the usual permutation operator, α and β are spin-up and spin-down functions. The singly excited singlet configurations are

$$V_{ik'} = 2^{-1/2} [(1\bar{1}, \cdots, i\bar{k}', \cdots) - (1\bar{1}, \cdots, \bar{i}k', \cdots)]. \quad (\text{B5})$$

Allowing configuration interaction, gives the functions

$$\Psi_a = A_{1a} V_1 + A_{2a} V_2 + \cdots. \quad (\text{B6})$$

The coefficients for normalized linear combinations of configurations used to construct the ground and two lowest-energy even-parity states are given in Table VI.

APPENDIX C: MATRIX ELEMENTS

In calculating transition rates and exciton energies, one requires matrix elements of the form

$$M_{\mu\nu}(\alpha\beta) = \int \Phi_\mu(\mathbf{r}) r_\alpha r_\beta \Phi_\nu(\mathbf{r}) d\mathbf{r}, \quad (\text{C1})$$

where μ, ν are the set of quantum numbers identifying the states of the free molecule, r_α and r_β stand for $x, y,$ or z in the molecular basis set. Along with $\mathbf{r}, r_\alpha,$ and r_β are 14-electron coordinates. Thus in one-electron language

$$M_{\mu\nu}(\alpha\beta) = \sum_{i,j=1}^{14} \int \Phi_\mu(\mathbf{r}_1 \cdots \mathbf{r}_{14}) \times r_{\alpha i} r_{\beta j} \Phi_\nu(\mathbf{r}_1 \cdots \mathbf{r}_{14}) \prod_{m=1}^{14} d\mathbf{r}_m. \quad (\text{C2})$$

We must treat matrix elements with $i=j$, one-electron integrals, and $i \neq j$, two-electron integrals. Since $\Phi_\mu(\mathbf{r}_1 \cdots \mathbf{r}_{14})$ are linear combinations of Slater determinants of one-electron functions, the rules for reducing the problem to the evaluation of one-electron, one-center integrals are well-known and present difficulties only in bookkeeping. The results are given in Table VII.

TABLE VII. The integrals $\int \Phi_\mu F_m \Phi_\nu d\tau$ for anthracene. All are in units of a_0^2 .

F_m	$A_{1g} - A_{1g}$	$A_{1g} - A_{1g}^*$	$A_{1g} - B_{1g}^*$	$A_{1g}^* - A_{1g}^*$	$B_{1g}^* - B_{1g}^*$
z^2	6.23	0	0	6.23	6.23
x^2	26.48	-1.22	0	28.79	76.43
y^2	12.92	1.03	0	16.47	14.89
xy	0	0	7.79	0	0

The wave functions are those of Appendix B. The matrix elements are calculated through direct application of Eqs. (9)–(13) in Ref. 15 by formally identifying our one- and two-electron operators with his, although the operators themselves are different.³⁰ Finally, all integrals reduce to two types. First, there are linear combinations of the coordinates of the atoms. We have used regular hexagons for anthracene with the inter-

³⁰ There are two typographical errors in the section of Ref. 15 we use: in Eq. (11) there are two terms “ $-[ij|ii]$ ”; one of them should be changed to read “ $-[ij|jj]$ ”. Then, in Eq. (12): $\sum_{f \neq i, l, v}$ should be changed to read $\sum_{f \neq i}$.

atomic distance taken as the average of the measurements of Sinclair *et al.*³¹ There are also integrals of the type

$$\int x^2 |\chi(\mathbf{r})|^2 d\mathbf{r},$$

which are matrix elements involving the coordinates of the $2p\pi$ carbon electron about its own nucleus. For these we used the Slater functions suggested by Pariser.

³¹ V. C. Sinclair, J. M. Robertson, and A. M. Mathieson, *Acta Cryst.* **3**, 251 (1950).

Theory of X-Ray Satellites

TEIJO ÅBERG

Laboratory of Physics, Institute of Technology, Otaniemi, Finland

(Received 16 November 1966)

A general theory has been developed with regard to x-ray excitations, based on the method of the sudden approximation. As one application, the production probabilities of all the normal single-hole x-ray states of F^- , Ne, Na^+ , Cl^- , Ar, and K^+ have been calculated in a self-consistent-field approximation. These production probabilities have been employed for derivation of the KL -satellite intensity values 36.5% (F^-), 21.1% (Ne), and 14.3% (Na^+) relative to the $K\alpha_{1,2}$ line and the KM -satellite intensity values 39.7% (Cl^-), 26.2% (Ar), and 19.3% (K^+) relative to the $K\beta_{1,3}$ line. In calculation of the relative satellite intensities, account has been taken of the difference between the oscillator strengths of the main line and the satellites, and the decay of KL to the KM states of Cl^- , Ar, and K^+ . It has further been shown that the exchange probabilities can be ignored in these calculations. The satellite intensities calculated display close agreement with the experimental intensities obtained from Deslattes's measurements as concerns Cl^- and Ar, although there is a slight disagreement in the case of K^+ . It has been suggested that the usual criterion of validity for sudden approximation need not be fulfilled exactly in applications, and a connection between the sudden-approximation probability and the dipole-transition probability has been found. In conclusion, there is a discussion of solid-state effects on the satellite intensities.

I. INTRODUCTION

CONCLUSIONS with respect to the origin of x-ray satellites are almost entirely based upon calculations of the energy positions of the x-ray satellites.¹ However, in this paper, consideration is given to calculation of the relative intensity of the satellites and the main line with the aid of the sudden approximation. The change in the Hamiltonian attributable to the production of an inner vacancy or hole is then regarded as a sudden perturbation.

The possibility of treating x-ray excitation by means of the sudden approximation seems to have first been indicated by Bloch.² Parrat and Schnopper^{3,4} have discussed the subject qualitatively in connection with the relaxation of an electron system after the formation

of an inner hole. Recently, Sachenko and Demekhin⁵ and the author⁶ have presented some satellite-intensity calculations based upon the sudden approximation. Richtmeyer⁷ studied the electron excitation of initial states of satellites in the Born approximation. This work continues the study of the sudden-approximation method, and presents the general theory with some new applications.

Related applications of the sudden approximation include calculations of auto-ionization rates of the atom in beta decay,^{8–10} calculations of the shake-off rates in charge spectra induced by x rays in noble-gas atoms,^{11–13}

¹ See, for example, D. J. Candlin, *Proc. Phys. Soc. (London)* **A68**, 322 (1955); Z. Horak, *ibid.* **A77**, 980 (1961); R. D. Deslattes, *Phys. Rev.* **133**, A399 (1964).

² F. Bloch, *Phys. Rev.* **48**, 187 (1935).

³ L. G. Parrat, *Rev. Mod. Phys.* **31**, 616 (1959).

⁴ H. W. Schnopper and L. G. Parrat, in *Röntgenspektren und Chemische Bindung*, edited by A. Meisel (VEB Reprocolor, Leipzig, 1966), p. 314.

⁵ V. P. Sachenko and V. F. Demekhin, *Zh. Eksperim. i Teor. Fiz.* **49**, 765 (1965) [English transl.: *Soviet Phys.—JETP* **22**, 532 (1966)].

⁶ T. Åberg, *Licenciate thesis*, University of Helsinki, 1966 (unpublished).

⁷ R. D. Richtmeyer, *Phys. Rev.* **49**, 1 (1936).

⁸ A. B. Migdal, *J. Phys. USSR* **4**, 449 (1941).

⁹ E. L. Feinberg, *J. Phys. USSR* **4**, 424 (1941).

¹⁰ J. S. Levinger, *Phys. Rev.* **90**, 11 (1953).

¹¹ T. A. Carlson, *Phys. Rev.* **130**, 2361 (1963).

¹² T. A. Carlson and M. A. Krause, *Phys. Rev.* **137**, A1655 (1965).

¹³ T. A. Carlson and M. A. Krause, *Phys. Rev.* **140**, A1057 (1965).